

An ultrasensitive and multispectral refractive index sensor based on quad-supercell metamaterials

Shuyuan Xiao¹, Tao Wang^{1,*}, Yuebo Liu², Xu Han¹, and Xicheng Yan¹

¹Wuhan National Laboratory for Optoelectronics, Huazhong University of Science and Technology, Wuhan 430074, People's Republic of China

²School of information and Optoelectronic Science and Engineering, South China Normal University, Guangzhou 510006, People's Republic of China

*wangtao@hust.edu.cn

Abstract: Plasmonic metamaterials support the localized surface plasmon resonance (LSPR) and the strong field enhancement could be applied to ultrasensitive biochemical sensing. In this work, a novel design of quad-supercell metamaterials of split ring resonators (SRRs) is proposed and simultaneous excitations of odd ($N=1$ and $N=3$) and even ($N=2$) resonance modes are realized due to additional asymmetry from the rotation with respect to the excitation field. The full utilization of these three resonance dips show bright prospects for multispectral application. As a refractive index (RI) sensor, ultrahigh sensitivities $\sim 1000\text{nm}/\text{RIU}$ for LC mode ($N=1$) and $\sim 500\text{nm}/\text{RIU}$ for plasmon mode ($N=2$) are obtained in near infrared (NIR) spectrum.

© 2018 Optical Society of America

OCIS codes: (160.3918) Metamaterials; (240.6680) Surface plasmons; (280.1415) Biological sensing and sensors.

References and links

1. C. M. Soukoulis, S. Linden, and M. Wegener, "Negative refractive index at optical wavelengths," *Science* **315**(5808), 47-49 (2007).
2. V. M. Shalaev, "Optical negative-index metamaterials," *Nat. Photonics* **1**(1), 41-48 (2007).
3. N. Liu, L. Langguth, T. Weiss, J. Kstel, M. Fleischhauer, T. Pfau, and H. Giessen, "Plasmonic analogue of electromagnetically induced transparency at the Drude damping limit," *Nat. Mater.* **8**(9), 758-762 (2009).
4. D. Schurig, J. J. Mock, B. J. Justice, S. A. Cummer, J. B. Pendry, A. F. Starr, and D. R. Smith, "Metamaterial Electromagnetic Cloak at Microwave Frequencies," *Science* **314**(5801), 977-980 (2006).
5. C. Wu, A. B. Khanikaev, and G. Shvets, "Broadband Slow Light Metamaterial Based on a Double-Continuum Fano Resonance," *Phys. Rev. Lett.* **106**(10), 107403 (2011).
6. Y. Li, L. Su, C. Shou, C. Yu, J. Deng, and Yu Fang, "Surface-enhanced molecular spectroscopy (SEMS) based on perfect-absorber metamaterials in the mid-infrared," *Sci. Rep.* **3**, 2865 (2013).
7. N. Liu, T. Weiss, M. Mesch, L. Langguth, U. Eigenthaler, M. Hirscher, C. Sönnichsen, and H. Giessen, "Planar Metamaterial Analogue of Electromagnetically Induced Transparency for Plasmonic Sensing," *Nano Lett.* **10**(4), 1103C1107 (2009).
8. B. X. Wang, X. Zhai, G. Z. Wang, W. Q. Huang, and L. L. Wang, "A novel dual-band terahertz metamaterial absorber for a sensor application," *J. Appl. Phys.* **117**(1): 014504 (2015).
9. E. Hutter, J. H. Fendler, "Exploitation of localized surface plasmon resonance," *Adv. Mater.* **16**(19), 1685-1706 (2004).
10. L. Tong, H. Wei, S. Zhang, and H. Xu, "Recent advances in plasmonic sensors," *Sensors* **14**(5), 7959-7973 (2014).
11. W. N. Hardy and L. A. Whitehead, "Split-ring resonator for use in magnetic resonance from 200-2000 MHz," *Rev. Sci. Instrum.* **52**(2), 213-216 (1981).

12. Q. Zhang, X. Wen, G. Li, Q. Ruan, J. Wang, and Q. Xiong, "Multiple Magnetic Mode-Based Fano Resonance in Split-Ring Resonator/Disk Nanocavities," *ACS Nano* **7**(12), 11071-11078 (2013).
13. W. Wang, Y. Li, J. Chen, Z. Chen, J. Xu, and Q. Sun, "Plasmonic analog of electromagnetically induced transparency in planar metamaterials: manipulation and applications," *J. Mod. Optic.* **61**(20), 1679-1684 (2014).
14. W. Wang, Y. Li, J. Peng, Z. Chen, J. Qian, J. Chen, J. Xu, and Q. Sun, "Polarization dependent Fano resonance in a metallic triangle embedded in split ring plasmonic nanostructures," *J. Optics.* **16**(3), 035002 (2014).
15. L. Zhu, F. Y. Meng, L. Dong, Q. Wu, B. J. Che, J. Gao, J. H. Fu, K. Zhang, and G. H. Yang, "Magnetic metamaterial analog of electromagnetically induced transparency and absorption," *J. Appl. Phys.* **117**(17), 17D146 (2015).
16. D. R. Smith, J. B. Pendry, and M. C. K. Wiltshire, "Metamaterials and negative refractive index," *Science*, **305**(5685), 788-792 (2004).
17. S. Han, R. Singh, L. Cong, and H. Yang, "Engineering the fano resonance and electromagnetically induced transparency in near-field coupled bright and dark metamaterial," *J. Phys. D* **48**(3), 035104 (2015).
18. S. Linden, C. Enkrich, M. Wegener, J. Zhou, T. Koschny, and C. M. Soukoulis, "Magnetic Response of Metamaterials at 100 Terahertz," *Science*, **306**(5700), 1351-1353 (2004).
19. R. Singh, C. Rockstuhl, F. Lederer, and W. Zhang, "Coupling between a dark and a bright eigenmode in a terahertz metamaterial," *Phys. Rev. B* **79**(8), 085111 (2009).
20. R. Singh, I. Al-Naib, M. Koch, and W. Zhang, "Sharp Fano resonances in THz metamaterials," *Opt. Express* **19**(7), 6312-6319 (2011).
21. I. Al-Naib, Y. Yang, M. M. Dignam, W. Zhang, and R. Singh, "Ultra-high Q even eigenmode resonance in terahertz metamaterials," *Appl. Phys. Lett.* **106**(1), 011102 (2015).
22. A. W. Clark, A. K. Sheridan, A. Glidle, D. R. S. Cumming, and J. M. Cooper, "Tunable visible resonances in crescent shaped nano-split-ring resonators," *Appl. Phys. Lett.* **91**(9), 093109 (2007).
23. X. Xu, B. Peng, D. Li, J. Zhang, L. M. Wong, Q. Zhang, S. Wang, and Q. Xiong, "Flexible visible-infrared metamaterials and their applications in highly sensitive chemical and biological sensing[J]. *Nano letters*," *Nano lett.* **11**(8), 3232-3238 (2011).
24. L. Y. M. Tobing, L. Tjahjana, D. H. Zhang, Q. Zhang, and Q. Xiong, "Deep subwavelength fourfold rotationally symmetric split-ring-resonator metamaterials for highly sensitive and robust biosensing platform," *Sci. Rep.* **3**, 2437 (2013).
25. L. Y. M. Tobing, L. Tjahjana, D. H. Zhang, Q. Zhang, and Q. Xiong, "Sub-100-nm sized silver split ring resonator metamaterials with fundamental magnetic resonance in the middle visible spectrum," *Adv. Opt. Mater.* **2**(3), 280-285 (2014).
26. C. Rockstuhl, F. Lederer, C. Etrich, T. Zentgraf, J. Kuhl, and H. Giessen, "On the reinterpretation of resonances in split-ring-resonators at normal incidence," *Opt. Express* **14**(19), 8827-8836 (2006).
27. P. B. Johnson and R. W. Christy, "Optical constants of the noble metals," *Phys. Rev. B* **6**(12), 4370 (1972).
28. E. D. Palik, "Ag (Silver)," in *Handbook of optical constants of solids*, (Academic press, New York, 1998).
29. N. Liu and H. Giessen, "Coupling effects in optical metamaterials," *Angew. Chem. Int. Edit.* **49**(51), 9838-9852 (2010).
30. C. Rockstuhl, T. Zentgraf, H. Guo, N. Liu, C. Etrich, I. Loa, K. Syassen, J. Kuhl, F. Lederer and H. Giessen, "Resonances of split-ring resonator metamaterials in the near infrared," *Appl. Phys. B* **84**(1-2), 219-227 (2006).
31. H. Guo, N. Liu, L. Fu, H. Schweizer, S. Kaiser, and H. Giessen, "Thickness dependence of the optical properties of split-ring resonator metamaterials," *Phys. Stat. Sol. B* **244**(4), 1256-1261 (2007).

1. Introduction

Plasmonic metamaterials are artificially periodic structure of metallic nanoparticles much smaller than the corresponding operating wavelength[1, 2, 3]. A lot of novel electromagnetic phenomena with no analog in nature have been reported and employed to a great variety of potential applications as electromagnetic cloaking[4], slow-light effect[5], molecular spectroscopy[6], and ultrasensitive sensing[7, 8]. The underlying physical principles of these phenomena are often related to the localized surface plasmon resonance (LSPR), which come from the collective oscillation of free electrons and induce the local electromagnetic field enhancement[9, 10].

Split ring resonator(SRR), first introduced by Hardy and Whitehead to realize the high Q magnetic resonance in the frequency region 200-2000 MHz[11], is an analog of a LC -oscillator circuit where the crescent arc resembles the inductance (L) and the split serves as the capacitance (C). Noble metal based SRR supports the LSPRs and is often adopted as the basic building block of plasmonic metamaterials[12, 13, 14, 15]. As kind of a simple and elegant

structure, the SRR has a group of tuneable parameters, the morphology, the size and periodicity and the LSPRs are highly dependent on them. By adjusting these structure parameters, the LSPRs have been respectively demonstrated in microwave[16, 17], infrared[18] and terahertz regions[19, 20, 21], and those generated in the visible and near infrared (Vis-NIR) spectrum[22, 23, 24, 25] are of considerable interest in the field of ultrasensitive biochemical sensing since it is the exact portion of the spectrum most relevant to many biochemical molecules, such as proteins, glucose, and DNA. The fabrication of the corresponding 100-nm size or smaller SRRs, once considered as a key obstacle, has been realized by a robust electron beam lithography (EBL) with high contrast in recent years[24, 25].

The feature that the inefficient excitation of resonance modes due to the strong polarization dependence once impedes the full utilization of the SRR, i.e., when the electric field is parallel to its split, only the two odd resonance modes ($N=1$ and $N=3$) are excited, while only the single even resonance mode ($N=2$) emerges when the electric field is perpendicular to the split[22, 26]. To address this concern, we propose a novel design in this work, supercell metamaterials consisting of four SRRs that are mutually rotated in each unit cell, where the odd and even resonance modes are simultaneously excited. As for application in biochemical sensing, all the three resonance dips show clearly observable shifts with the slight increase in the refractive index (RI) of the surrounding environment. Especially, ultrahigh RI sensitivities $\sim 1000\text{nm}/\text{RIU}$ for LC mode ($N=1$) and $\sim 500\text{ nm}/\text{RIU}$ for plasmon mode ($N=2$) in NIR are obtained simultaneously and reveal bright prospects in multispectral sensing.

2. The quad-supercell metamaterials structure and numerical model

Fig. 1 schematically show three quad-supercells of the SRRs with different mutual rotation angles: 0° , 45° and 90° . Silver is adopted as the constituting metal of the SRRs due to its low optical loss and high plasma frequency. Each identical SRR has a size $s=100\text{nm}$, a width $w=20\text{nm}$, a thickness $h=30\text{nm}$ (thicker than the skin depth of silver $\sim 22\text{nm}$ [27]) and a split angle $\theta = 30^\circ$, and the lattice constant is $a=180\text{nm}$. The finite-difference time-domain method with the commercial software FDTD Solutions is employed here. The calculation step is fixed as $5\text{nm} \times 5\text{nm} \times 5\text{nm}$. The periodical boundary conditions with $p=500\text{nm}$ apply in both x and y directions, and perfectly matched layers in z direction are utilized along the propagation of light. It is noted that only the x-polarization planewave is employed since the same results should be obtained with the y-polarization planewave due to obvious rotational symmetric relations among these three arrays. The substrate is quartz with a RI of 1.4 and frequency-dependent optical properties of silver are extracted from Palik's data[28].

3. Simulation results and discussion

The simulated transmission spectra for the three different metamaterials arrays are shown in Fig. 2. As expected from the broken symmetry, the transmission spectra of the SRRs arrays show the strong polarization dependence. When the rotation angle is 0° and the electric field E is paralleled to the split, two resonance dips generated at 1615.19nm and 644.628nm are recognized as the LC ($N=1$) mode and quadrupole ($N=3$) mode, respectively. However, when the rotation angle is 90° , only a single resonance dip is generated at 785.235nm and it is identified as plasmon ($N=2$) mode. Amazing happens when the rotation angle turns to 45° , three resonance dips emerge at nearly the same wavelengths where $N=1$, $N=3$ and $N=2$ resonance dips previously located when the mutual rotation angle is 0° and 90° , respectively, suggesting both the odd ($N=1$, $N=3$) and the even ($N=2$) modes are excited simultaneously, which is previously forbidden due to the symmetry constraints of orthogonally rotational SRRs arrays.

In order to get insights into the underlying physical mechanism, the electric field enhancement and surface charge density distributions at resonances in the z plane are plotted in Fig.

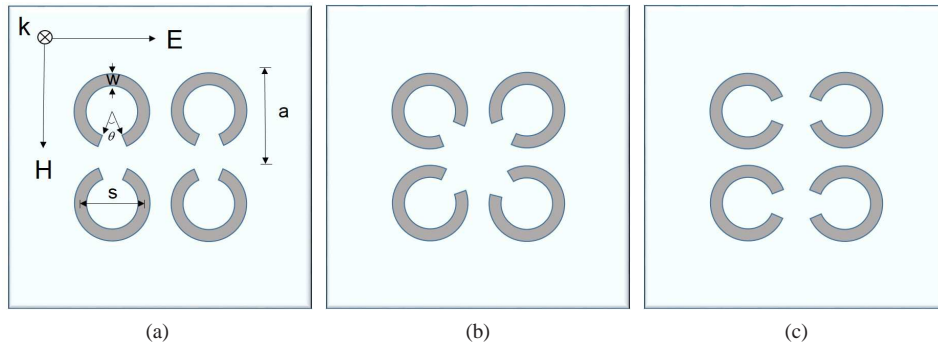


Fig. 1: Three quad-supercells of the SRRs with different mutual rotation angles; the SRRs are rotated around their centers with an angle: (a) 0° , (b) 45° , and (c) 90° .

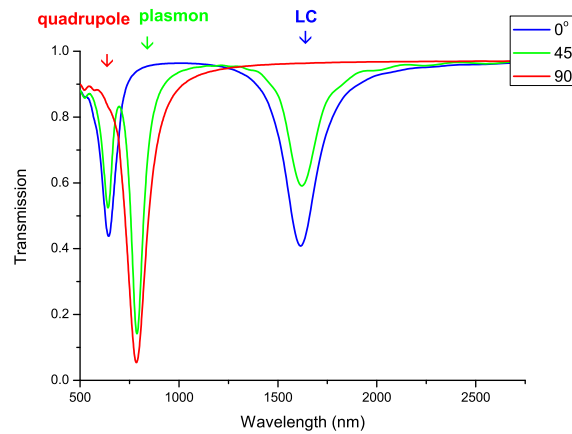


Fig. 2: Transmission spectra of metamaterials arrays with different mutual rotation angles: (a) 0° , (b) 45° and (c) 90° .

3 and 4. As indicated in Ref[22], the mode order is described as one minus the number of nodes, thus it is straightforward to confirm above-mentioned resonance modes show the characteristic behaviors of the $N=1$, $N=2$ and $N=3$ modes. As shown in Fig. 3(a) and Fig. 4(a), for the resonance dip at 1622.18nm ($N=1$), the electric field is mainly confined in the vicinity of the split and a strong circulating current in each SRR is observed, which validates its support for magnetic dipole response and could be understood in terms of a LC -oscillator circuit with the split serving as a capacitor. A typical electric dipole response, i.e., the plasmon mode, at 786.885nm ($N=2$) is clearly revealed in Fig. 3(b) and Fig. 4(b), the net induced dipoles in the quad-supercell exhibit a clear tendency to follow the polarization of the incoming planewave. And at the shortest resonance $\lambda=641.316\text{nm}$ ($N=3$), the quadrupole mode is also verified, and the electric field confinement as well as the surface charge density distributions shown in Fig. 3(c) and Fig. 4(c) are comparatively weak.

As for the potential application in biochemical sensing, it is significant that these LSPRs should be tuned to the corresponding wavelength, i.e., the Vis-NIR portion of the spectra. To achieve this, the effects of the structure parameters of the supercell metamaterials need to be

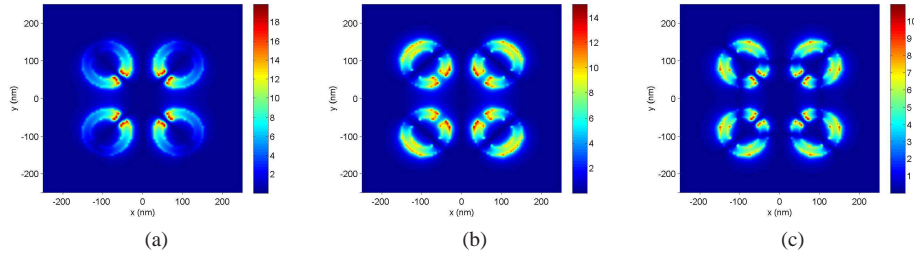


Fig. 3: Electric field enhancement at the angle of 45° of (a)*LC* mode ($N=1$), (b)plasmon mode ($N=2$) and (c)quadrupole mode ($N=3$).

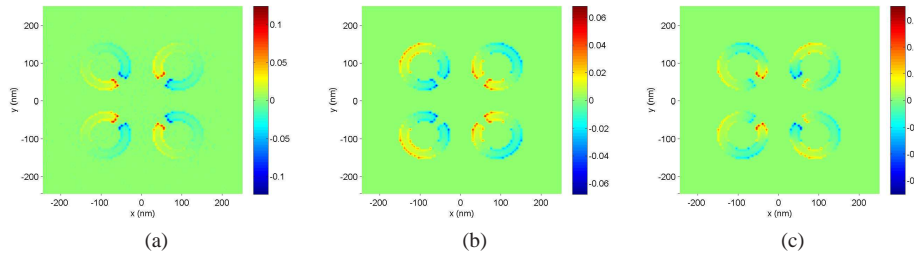


Fig. 4: Surface charge distribution at the angle of 45° of (a)*LC* mode ($N=1$), (b)plasmon mode ($N=2$) and (c)quadrupole mode ($N=3$).

investigated.

Fig. 5(a) shows the variation in offset transmission spectra for the quad-supercell metamaterials with different split angles. When θ changes from 45° to 15° , red shifts from 1523.19nm to 1767.71nm (for *LC* mode), from 778.702 nm to 795.242nm (for plasmon mode) and from 625.251nm to 666.429nm (for quadrupole mode) are observed. These phenomena are also directly reflected with the resonance wavelength as a function of split angle in Fig. 5(b) and that this parameter affect the *LC* resonance most while leave the other two modes nearly untouched can be well understood that nonsymmetrical current flow caused by the split leads to an increase in capacitance in *LC* circuit, and smaller split angle leads to a larger capacitance thus increases the resonance wavelength.

In Fig. 6(a)-(c) the offset transmission spectra of the quad-supercell metamaterials as a function of the change in the size and lattice constants are presented. For $a=200$ nm, when the size of the SRR decreases from 140nm to 60nm, the *LC* resonance exhibits clear blue shifts from 2678.11nm to 1236.46nm, the plasmon resonance from 1138.69nm to 609.971nm and the quadrupole resonance from 783.591nm to 564.025nm. For $a=180$ nm, as the SRR size decreases from $s = 140$ nm to $s = 60$ nm, blue shifts from 2129.69nm to 1236.46nm (for *LC* mode), from 1015.18nm to 609.971nm (for plasmon mode) and from 783.591nm to 563.177nm (for quadrupole mode) are observed. And for $a=160$ nm, with the size ranging from 140nm to 60nm, the *LC* resonance shifts from 2117.65nm to 1236.46nm, the plasmon resonance from 998.933nm to 607.99nm and the quadrupole resonance from 780.325nm to 564.025nm. An evident linear relation between the resonance wavelength and the size with each different lattice constant is clearly displayed in Fig. 6(d). The only notable exception arises when $s=140$ nm and $a=160$ nm, these four SRRs are tangent to each other and physically connected, thus the con-

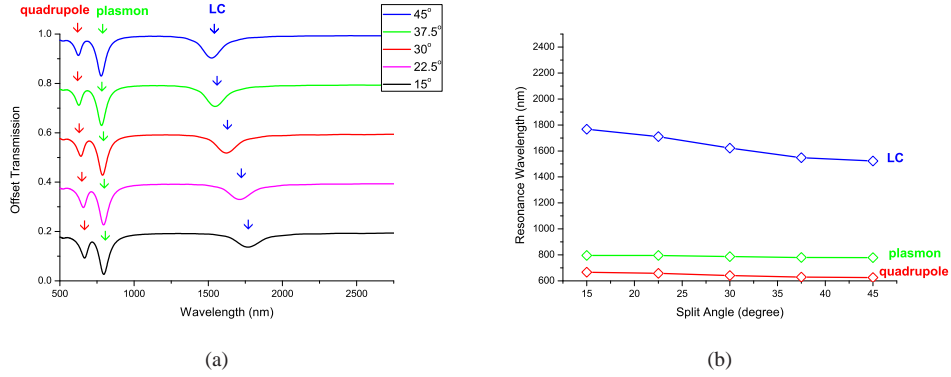


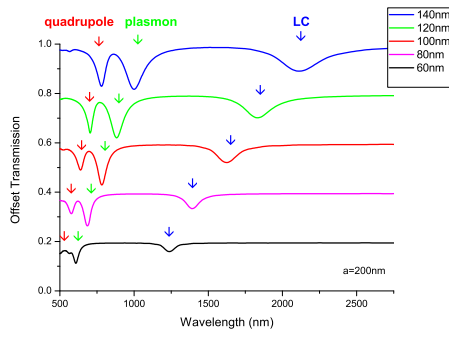
Fig. 5: (a) Offset transmission spectra and (b) resonance wavelengths for the quad-supercell metamaterials with different split angles.

ductive coupling plays a significant role and leads to much strong coupling strength[29]. As a result, the *LC* resonance shows a high redshift beyond NIR and we should abort this arrangement.

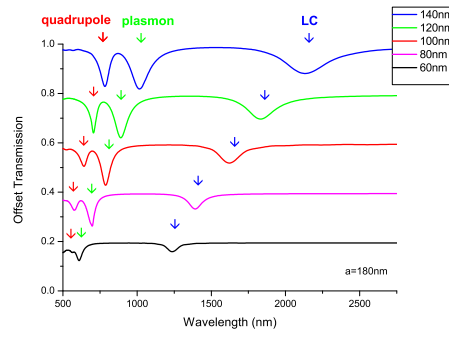
Moreover, the simulation on the effects of the width and thickness have been also performed, and the results in Fig. 7 confirms that the SRR exhibits longer resonance wavelength when the width (thickness) is narrower (smaller)[30, 31].

It is found that the above shifts of the *LC* mode and the plasmon mode almost cover the whole near infrared (NIR) spectrum, and these two resonance dips could be applied to multispectral sensing in NIR. The sensitivity is usually defined as the amount of peak(dip) shift per refractive index unit (RIU) change to characterize the performance of a SPR sensor[10]. In order to examine the sensitivity of our proposed RI sensor, the transmission spectra for the quad-supercell metamaterials with 100nm thick cover layer filled with water ($n=1.332$) (blue) and 25% aqueous glucose solution ($n=1.372$) (green) on the surface are respectively simulated. In Fig. 8, shifts of all the three resonance dips to longer wavelengths are clearly observed when the cover layer is filled with aqueous glucose solution instead of water due to the slight increase of the RI of surrounding environment. The wavelength shifts are 41nm (*LC* mode), 18nm (plasmon mode) and 12nm (quadrupole mode), which correspond to a set of sensitivities 1018nm/RIU, 446nm/RIU and 294nm/RIU.

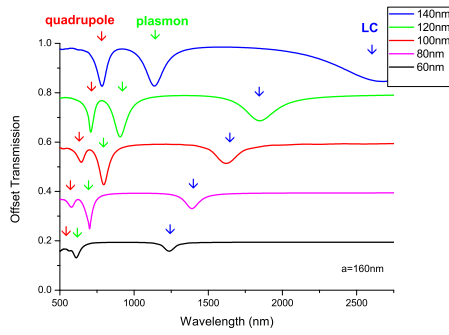
Now that the *LC* resonance mode wavelength depends on the cover layer permittivity ($\epsilon_c = n_c^2$) and the resonator size as $\lambda_{LC} \propto s(\epsilon_c)^{1/2}$, the sensitivity of *LC* mode should have a positive correlation with the size of the SRRs $S = d\lambda_{LC}/dn_c \propto s$ [24]. Therefore the effects of the size on the sensitivity have been investigated, for the largest SRRs with $s=140$ nm, the simulated spectrum shifts are 52.49nm (*LC* mode) and 22.67nm (plasmon mode), which correspond to 1312.25nm/RIU and 566.75nm/RIU, and for the smallest SRRs with $s=60$ nm, the shifts are 30.37nm (*LC* mode) and 9.23nm (plasmon mode), which correspond to 759.25nm/RIU and 232.13nm/RIU. The sensitivity as a function of the size is plotted in Fig. 9, in the near infrared spectrum (780~2526nm), the *LC* mode holds a considerably high sensitivity from ~1500nm to ~2200nm and reaches the maximum 1017nm/RIU within a 100nm-SRR quad-supercell, on the other hand, the plasmon also possesses a good sensitivity of 522nm/RIU around 1000nm within a 120nm-SRR quad-supercell.



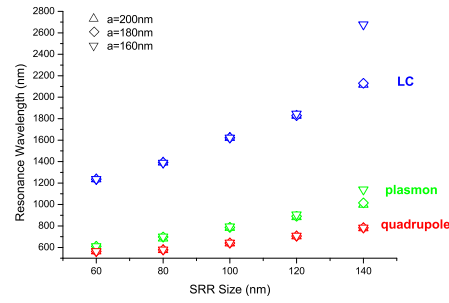
(a)



(b)

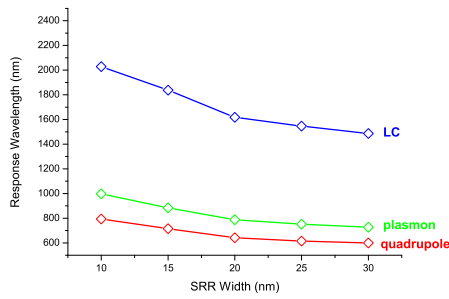


(c)

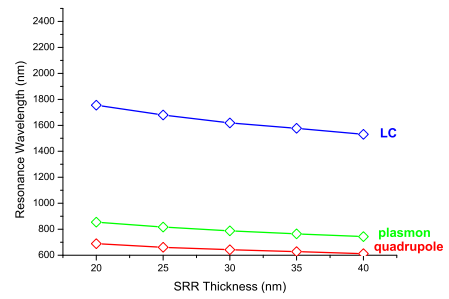


(d)

Fig. 6: (a)-(c) Offset transmission spectra and (d) resonance wavelengths for the quad-supercell metamaterials with different sizes and lattice constants.



(a)



(b)

Fig. 7: Resonance wavelengths for the quad-supercell metamaterials with different (a) widths and (b) thicknesses.

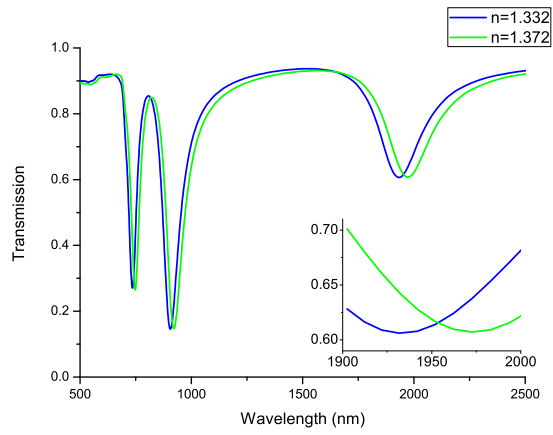


Fig. 8: The transmission spectra for the quad-supercell metamaterials by changing 100nm thick cover layer filled with water ($n=1.332$) to 25% aqueous glucose solution ($n=1.372$). Inset: enlarged figure of the shift of the transmission dip.

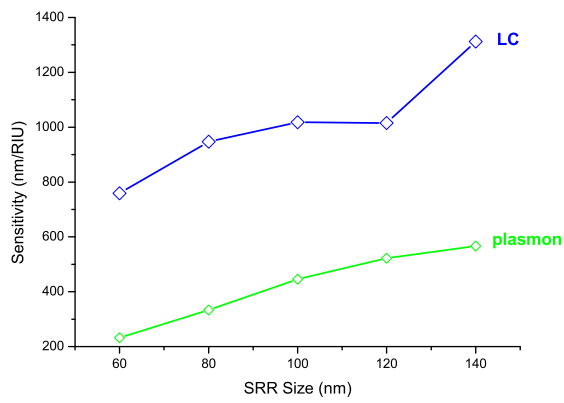


Fig. 9: Simulated sensitivity for the quad-supercell metamaterials with different sizes.

4. Conclusion

In conclusion, the simultaneous excitations of both the odd ($N=1$ and $N=3$) and even ($N=2$) resonance modes in SRRs, which are forbidden due to symmetry constraints, have been realized in our proposed quad-supercell metamaterials. In order to make better use of these LSPRs, the effects of structure parameters have also been systematically investigated and phenomenologically explained. Ultrahigh sensitivities $\sim 1000\text{nm/RIU}$ for *LC* mode ($N=1$) and $\sim 500\text{nm/RIU}$ for plasmon mode ($N=2$) are obtained in NIR spectrum and are expected to have bright prospects in ultrasensitive and multispectral biochemical sensing. Furthermore, the design principles we have introduced in this work could be applied to other geometries of metamaterial sensors across large parts of the electromagnetic spectrum.

Acknowledgments

The author Shuyuan Xiao expresses his deepest gratitude to his Ph.D. advisor Tao Wang for providing guidance during this project and also thank Dr. Qi Lin and Mr. Yao Jiang for beneficial discussion. This work is supported by the National Natural Science Foundation of China (Grant No. 61376055 and 61006045), and the National Basic Research Program of China (Grant No. 2010CB923204).